JAAS

PAPER

Cite this: *J. Anal. At. Spectrom.*, 2016, **31**, 1023

Precise measurement of stable potassium isotope ratios using a single focusing collision cell multi-collector ICP-MS†

Weiqiang Li,*[ab] Brian L. Beard[cd] and Shilei Li[e]

High precision potassium isotope ratio measurements were made using a collision-cell equipped single focusing Multi-Collector Inductively Coupled Plasma Mass Spectrometer (MC-ICP-MS). Interferences on ^{41}K from $^{40}ArH^+$ were largely suppressed through collision with He gas atoms, and reaction with H_2 or D_2 gas molecules in the collision cell under optimum collision gas flow conditions. Using H_2 or D_2 as the collision gas, we distinguish charged argon–deuterium molecules (ArD^+) generated in the collision cell from argon hydride (ArH^+) generated in the plasma or in the interface region (referred to as "plasma-related AH^+" hereafter), and demonstrate, for the first time, that both plasma-related and collision cell-generated ArH^+ are important sources of ArH^+ that interfere with $^{41}K^+$ in collision-cell ICP-MS instruments that use H_2 as a collision gas. The use of D_2 instead of H_2 as a reactive gas in the collision cell resulted in better overall performance in K isotope ratio measurements. By combining these mass spectrometry methods with chemical purification of K by ion exchange chromatography, we achieved an internal precision of $<\pm 0.07‰$ (2 standard error) and an external reproducibility of $<\pm 0.21‰$ (2 standard deviation, or 95% confidence) in the $^{41}K/^{39}K$ ratio measurement for geological and biological samples. With the improved precision, it is possible to distinguish a ~1.3‰ variation in K isotope compositions ($^{41}K/^{39}K$ ratios) among seawater, igneous rocks, and biological samples. The K isotope system is likely to be beneficial in providing a better understanding of potassium cycling during continental weathering and the uptake of nutrients by plants.

Received 14th December 2015
Accepted 16th February 2016

DOI: 10.1039/c5ja00487j

www.rsc.org/jaas

Introduction

Potassium is a major element in the earth's crust and oceans, and is an essential nutrient that plays a key role in a variety of metabolic and physiological processes in organisms. Potassium has three naturally occurring isotopes: stable ^{39}K (93.258%), radiogenic ^{40}K (0.012%, half-life 1.248 billion years), and stable ^{41}K (6.730%). Because of its ubiquitous occurrence, and the wide range of physical, chemical, geological, and biological processes involving K in nature, there has been strong interest in using variations in stable K isotope ratios to study K-cycling.

Attempts to perform $^{41}K/^{39}K$ ratio measurement using thermal ionization mass spectrometry (TIMS) date back to the 1960s.[1,2] However, because K has only three isotopes it is impossible to rigorously correct for instrumental mass fractionation from one sample to another using the double spike method, and thus the external precision was limited to a level of ±1‰ (ref. 3 and 4) for the $^{41}K/^{39}K$ ratio using TIMS methods, despite the fact that the internal precision for $^{41}K/^{39}K$ ratio measurement with modern TIMS can be well below 1‰.[5] In a novel attempt to avoid mass bias variability from filament to filament, K isotopes were analyzed by secondary ionization mass spectrometry (SIMS) of K samples that were fused into borate glass beads.[5,6] Using the SIMS method, external precision for the $^{41}K/^{39}K$ of ±0.5‰ was reported.[6,7] In previous TIMS and SIMS studies, over 8‰ variations in $^{41}K/^{39}K$ ratios have been reported from lunar soils[3,6] and microtektites.[8] These large variations in K isotope compositions occur in samples in which high temperature evaporation and/or condensation of K took place. Previous studies were not able to distinguish the small, naturally occurring mass-dependent (<1‰) variations that were thought to occur in terrestrial samples that had not been affected by evaporation or condensation.[6]

Inductively coupled plasma mass spectrometry (ICP-MS), with its efficient plasma ionization source that produces

[a]*State Key Laboratory for Mineral Deposits Research, School of Earth Sciences and Engineering, Nanjing University, Nanjing 210046, P. R. China. E-mail: liweiqiang@nju.edu.cn*

[b]*Lunar and Planetary Science Institute, Nanjing University, Nanjing 210046, P. R. China*

[c]*Department of Geoscience, University of Wisconsin-Madison, 1215W Dayton Street, Madison, Wisconsin 53706, USA*

[d]*NASA Astrobiology Institute, University of Wisconsin-Madison, Madison, Wisconsin, USA*

[e]*MOE Key Laboratory of Surficial Geochemistry, School of Earth Sciences and Engineering, Nanjing University, Nanjing 210046, P. R. China*

† Electronic supplementary information (ESI) available. See DOI: 10.1039/c5ja00487j

a constant instrumental mass bias, provides an alternative method for K isotope measurement. Depending on instrument setting and analysis conditions, the precision of a single collector ICP-MS for K isotope measurement varied from ±3‰ to ±10‰,[9–12] limiting its applications to enriched ^{41}K tracer studies in biological and nutrition sciences.The advent of a magnet-sector multi-collector ICP-MS (MC-ICP-MS) since the late 1990s has enabled measurements of isotopic ratios of many metal elements such as Mg, Cu, and Fe with precisions better than ±0.1‰.[13] This new instrumentation led to a mushrooming in application of new isotope systems to various geochemical, biogeochemical, and environmental problems.[14] Precise measurement of K isotope ratios using MC-ICP-MS, however, remains highly challenging because the Ar plasma generates argide isobars on the K mass spectrum including $^{40}Ar^+$ and $^{40}ArH^+$ on ^{40}K and ^{41}K respectively. Because we are only concerned with making precise and accurate $^{41}K/^{39}K$ ratios we do not discuss in detail methods to suppress $^{40}Ar^+$ isobars to a level suitable for analysis of K isotope ratios with ^{40}K. Previous MC-ICP-MS using double focusing instruments have attempted to minimize argide isobars using cool plasma techniques, and decrease the width of the ion beam to improve mass resolution and avoid argide isobars.[15,16] Combining these methods, precise K isotope analyses, with an internal precision of ±0.05‰ in $^{41}K/^{39}K$ ratios, have been reported in several recent conferences.[15,16] Although application of cold plasma does not necessarily decrease sensitivity for K in ICP instruments within certain power ranges,[11,17] high mass resolution mode decreases instrument sensitivity by an order of magnitude, which requires larger quantities of K for an analysis, and thus is undesirable in studies of small or precious samples, such as many biological or extra-terrestrial samples.

In contrast to a double focusing MC-ICP-MS, a single focusing MC-ICP-MS (*e.g.*, Micromass IsoProbe) uses a collision (reaction) cell with a thermalizing gas such as Ar or He to minimize the energy spread of the ion beam and reactive gasses, such as H_2, to suppress unwanted argide isobars. Suppression of argide isobars by a collision cell offers an alternative approach for high precision K isotope analysis using MC-ICP-MS. Measurement of $^{41}K/^{39}K$ ratios using a collision cell MC-ICP-MS (Micromass IsoProbe) has been reported in recent studies on high temperature experiments,[18,19] in which an external precision of ±0.3‰ was achieved. However, the technical details for high precision $^{41}K/^{39}K$ ratio measurement were little discussed in the two studies,[18,19] and it was not known whether further improvement of analytical precision is attainable. In addition, data in the two studies were the products of experimental studies designed to evaluate the degree of K isotope fractionation associated with high temperature evaporation or diffusion.[18,19] These studies neither reported K isotope data on natural samples nor did they evaluate the amount of ArH^+ produced with H_2 gas in the collision cell.

In this contribution, we report details of K isotope measurement using a single focusing MC-ICP-MS (Micromass IsoProbe) that was equipped with a hexapole collision cell. We take advantage of the collision cell to largely suppress the plasma-related ArH^+ which minimizes isobaric interference on ^{41}K isotopes, and magnet sector multi-collection of the K mass spectrum to achieve high precision $^{41}K/^{39}K$ isotope ratio measurements. Importantly, we address the potential problem of ArH^+ production in a collision cell by replacing the commonly used H_2 gas with high purity D_2 gas as the reaction gas; so the argon hydride product from an ion–molecule reaction in the collision cell has a m/z of 42 (ArD^+) and does not interfere with ^{41}K. Additionally, use of H_2 or D_2 gas in the collision cell allows us to trace the relative proportion of argon hydride generated before the collision cell *versus* that in the collision cell, which advances our understanding of the ion–molecule reaction in the widely used collision/reaction cell in quadrupole ICP-MS. We demonstrate that an external precision better than ±0.21‰ (2 standard deviation, or ~95% confidence level) in $^{41}K/^{39}K$ ratio measurement can be achieved for geological and biological samples, and it is possible to distinguish natural variations in K isotope compositions in terrestrial samples.

Experimental

Chemical procedure

All chemical procedures were performed in laminar flow hoods (class 100, or ISO class 5) in a clean room (class 1000, or ISO class 6) with HEPA filtered air at Nanjing University. Teflon coated hot plates, Teflon beakers, double distilled reagents, and deionized (18.2 MΩ) water were used throughout the experiments to minimize contamination.

Silicate samples (10–50 mg) were digested using 2 mL of a 1 : 1 mixture of concentrated HNO_3 and HF in tightly capped Teflon beakers, heated overnight on a hotplate at 130 °C, and then evaporated to dryness at 99 °C. The dissolution procedure was repeated until all the silicate material was digested. Following dissolution, samples were dissolved in 5 mL of 6 mol L^{-1} HCl. Biological samples were ashed in pre-cleaned quartz crucibles in a muffle furnace at 600 °C for 5 hours. The ashed samples were transferred into 15 mL centrifuge tubes, and soaked in 10 mL of 0.5 mol L^{-1} HNO_3 for at least 2 days; the K-containing leachates were separated using centrifugation followed by filtration using 0.22 μm syringe filters. Water samples were evaporated to dryness at 99 °C and then dissolved in 2 mL of 0.5 mol L^{-1} HNO_3. Typically an aliquot of the dissolved sample that contained 50–200 μg of K was transferred into a new beaker and evaporated to dryness, then re-dissolved in 50–100 μL concentrated HNO_3 and heated to dryness. The nitric acid fluxing procedure was repeated three times to ensure that nitrate was the predominant anion. The sample was then dissolved in 0.5 mL of 1.5 mol L^{-1} HNO_3 and was loaded on a cation exchange resin to purify K.

Separation of K from matrix elements in geological and biological samples was achieved using a two stage column procedure (Fig. 1, Appendix†). The first stage column used 1 mL volume of 100–200 mesh BioRad® AG50W-x12 resin and 1.5 mol L^{-1} HNO_3 as the eluent, and separated K from bulk Na, Al, and Ca (Fig. 1A). The second stage column used a 0.4 mL volume of 100–200 mesh BioRad® AG50W-x8 resin and three different acids, to achieve complete separation of K from Mg, and Ti, and

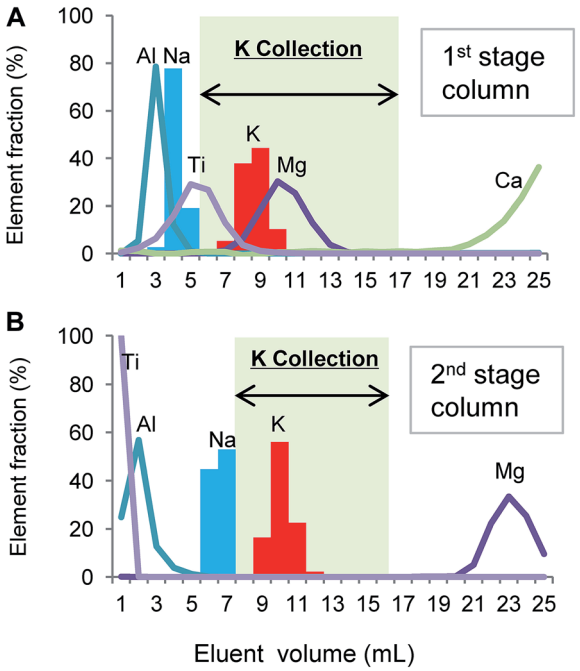

Fig. 1 Elution curves for major matrix elements in geological and biological samples. Details of the ion exchange columns and elution procedures are provided in the Appendix.†

performed additional removal of any Na, Al, and Ca in the sample after the 1st stage column (Fig. 1B). The recovery of K was 99.4 ± 2.1% (2 standard deviation, $n = 54$), and the total procedural blank of K was 3–8 ng ($n = 5$).

Mass spectrometry

Isotopic analysis of K was performed using a Micromass IsoProbe MC-ICP-MS housed at the University of Wisconsin–Madison. The instrument was run with a standard 1350 W forward RF power at standard mass resolution (~400 resolving power) using He (99.999% purity from Air Gas Products) as the collision gas and ultrapure H_2/D_2 gas (99.999% H semi-conductor research grade from Air Gas Products and 99.8% D from Cambridge Isotope Laboratories, respectively) as the reaction gas; the collision cell was operated at 6 MHz. Ion signals were simultaneously collected at m/z 39, 40, 41 and 42. A 10^{10} Ω resistor was used for the Faraday cup signals on mass number 39, and 10^{11} Ω resistors were used for the Faraday cup signals on other mass numbers. Potassium solutions were introduced to the Ar plasma using a self-aspirating Glass Expansion Micromist nebulizer with an uptake rate of ~100 μL min^{-1} and a Glass Expansion Cyclonic spray chamber cooled to 5 °C using a water jacket. Membrane desolvation (dry plasma) was not used to ensure effective washout between analyses. More details of the mass spectrometer settings are provided in the Appendix.† Using the above protocols and the optimum collision gas flow conditions (detailed in the following section), a 1 ppm K solution produced a typical signal intensity of 7–11 V (10^{10} Ω resistor but amplifier bias was corrected by a factor of 10 by instrument software during analysis) for mass 39, and 0.6–1 V (10^{11} Ω resistor) for mass 41; and clean 0.1% nitric acid produced "on-peak" blanks of <1 mV at mass 39 and <0.4 mV at mass 41, respectively.

Potassium isotope ratios were determined using a standard-sample-standard bracketing method. A 1 ppm in-house K stock solution (UW-K) was used as the bracketing standard, and sample solutions (including all test solutions) were typically diluted to 1 ± 0.1 ppm for analysis. Prior to each isotopic analysis, a 60 s on-peak acid blank was measured and subtracted from the analyte signal. Each isotopic analysis consisted of forty 5 second integrations. This routine results in a typical internal (2 standard error) precision better than ±0.07‰ in a $^{41}K/^{39}K$ ratio.

Potassium isotope compositions are reported using the standard per mil (‰) notation of $\delta^{41}K$ for a $^{41}K/^{39}K$ ratio, where

$$\delta^{41/39}K = [(^{41}K/^{39}K_{sample})/(^{41}K/^{39}K_{standard}) - 1] \times 1000$$

All K isotope ratios are reported relative to NIST SRM 3141a; the in-house K isotope standard UW-K has a $\delta^{41}K$ value of −0.12 ± 0.21‰ (2SD, $n = 43$) relative to NIST SRM3134a; the 2-sigma uncertainty of the a $\delta^{41}K$ value measurement is therefore estimated at ±0.21‰.

Collision cell gas flow and argon hydride cancellation/generation

The IsoProbe collision cell has three gas inlets, each with its own mass flow controller, which allow up to 10 mL min^{-1} flow for each of Ar, He, and H_2 gases. Use of Ar as the collision gas seriously deteriorates sensitivity on K and was abandoned; instead a set of experiments were carried out to test the influence of He and H_2/D_2 gases on Ar hydride suppression and production. The gas flow settings for each experiment are tabulated in Table 1. In these experiments, a clean 0.1% HNO_3 acid was aspirated into the mass spectrometer under different collision cell gas flow conditions, and Faraday cup signals on masses 39, 40, 41, and 42 were simultaneously measured to monitor signals of ^{39}K, $^{40}Ar^+$, $^{40}ArH^+$, and $^{40}ArD^+$, respectively. Additionally, sensitivity for K under different collision gas conditions was monitored by ^{39}K signals while aspirating a 1 ppm K solution into the MC-ICP-MS. The results are plotted in Fig. 2, and raw data are provided in the Appendix.†

Table 1 Summary of experiments for testing collision cell gas flow conditions

Experiment ID.	He gas flow (mL min^{-1})	H_2 gas flow (mL min^{-1})	D_2 gas flow (mL min^{-1})
H_2-a	1–10	5 (Fixed)	—
H_2-b	10 (Fixed)	0.9–7	—
D_2-a	1–10	—	5 (Fixed)
D_2-b	1–10	—	2 (Fixed)
D_2-c	1–10	—	1 (Fixed)
D_2-d	10 (Fixed)	—	0.5–7

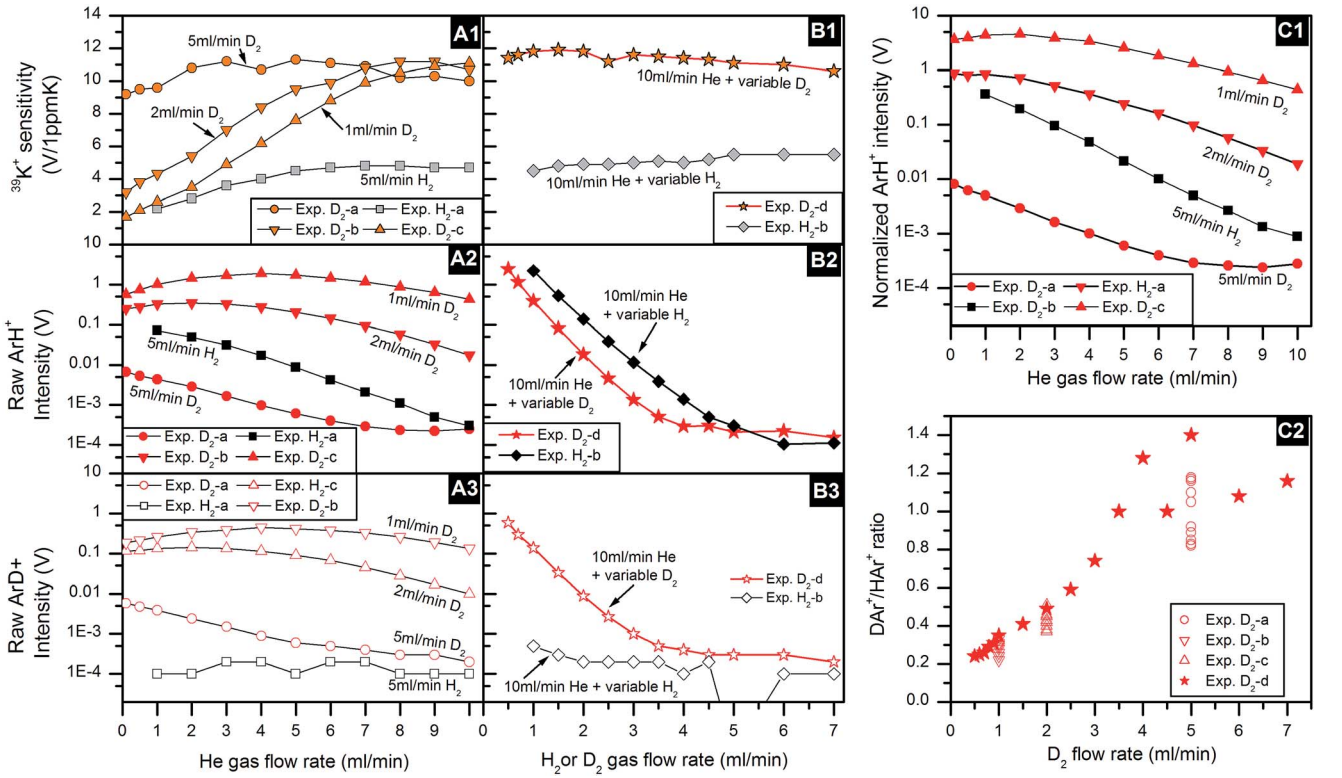

Fig. 2 Intensities of $^{39}K^+$ (A1 and B1) for a 1 ppm solution, and intensities of $^{40}ArH^+$ (A2 and B2) and $^{40}ArD^+$ (A3 and B3) for a clean 0.1% HNO_3 solution under different collision gas flow conditions, K sensitivity normalized ArH^+ intensity (C1) for a clean 0.1% HNO_3 solution under different collision gas flow conditions and $^{40}ArD^+/^{40}ArH^+$ ratios under different gas flow conditions (C2). For details, see Table 1 and Appendix.†

Ar^+ is efficiently suppressed by H_2 or D_2 even at flow rates as low as 1 mL min^{-1}, where the Ar^+ signal is always below 10 mV (Appendix†); experiments using D_2 yielded consistently lower Ar^+ signals than those using H_2 gas (Appendix†). It should be noted that even mV level Ar^+ is still too large to allow valid $^{40}K/^{39}K$ ratio measurements. Suppression of ArH^+ was less efficient under low collision gas flow conditions. When H_2 or D_2 flow was at 1 mL min^{-1}, the ArH^+ signal was on the order of volts or higher which would swamp the $^{41}K^+$ signal. Both He and H_2/D_2 gases suppressed the ArH^+ molecules. The effects of He may include collision-induced dissociation,[20] and increase in the ion–molecule interaction chance, by increasing the residence time in the collision cell.[21] Nonetheless, obviously H_2/D_2 has the primary effect in suppressing ArH^+ (Fig. 2, plots A2, B2 and C1), due to the reaction of proton transfer[22] that takes place in the reaction cell:

$$ArH^+ + H_2 \text{ (or } D_2) \rightarrow H_3^+ \text{ (or } HD_2^+) + Ar \quad (1)$$

In experiments that used D_2 as the reaction gas, signals of ArD^+ (mass: 42) were clearly identified, particularly under low D_2 and low He conditions (Fig. 2, plots A3 and B3); in contrast, ion signals of ArD^+ (mass 42) were very low in experiments that used H_2 as the reaction gas, almost at the detection limit of sub-mV, even under low H_2 and low He conditions. These facts indicate that the large ArD^+ polyatomic ion signals are produced in the reaction cell containing D_2, most likely *via* an atom transfer reaction:[22]

$$Ar^+ + D_2 \rightarrow ArD^+ + D \quad (2)$$

Therefore, in an instrument that used conventional H_2 gas as a reaction gas, ArH^+ produced through atom transfer in the collision cell is another source of ArH^+ in addition to plasma-related ArH^+. It should be noted that both ArH^+ and ArD^+ signals decreased with increasing H_2 or D_2 gas flow (Fig. 2, plots A2, B2, A3, B3 and C1), suggesting that the proton transfer reaction (reaction (1)) outpaced the atom transfer reaction (reaction (2)) in the collision cell at higher H_2/D_2 gas flow, although such an interpretation requires further work on reaction constants for the two types of reactions.

The experimental settings in this study allow a novel way to quantify the relative contributions of plasma-related argon hydride and collision cell generated argon hydride in collision cell ICP instruments, *via* measurement of ArH^+/ArD^+ ratios in Exps D_2-a, b, c, d. As shown in plot C2 of Fig. 2, the ArD^+/ArH^+ ratio decreased from ~1 to ~0.2, as the D_2 gas flow rate decreased from 7 mL min^{-1} to less than 1 mL min^{-1}, and such a trend did not correlate with variations in He gas flow, all supporting the prominent role of H_2/D_2 gas in concurrent generation and cancellation of argon hydride (or ArD^+) in the collision cell. The relatively large scatter in the ArD^+/ArH^+ ratio at a high D_2 gas flow rate (>4 mL min^{-1}, Fig. 2, plots C2) is attributed to the low (sub mV) ArD^+ and ArH^+ signals (Fig. 2, plots B2 and B3).

Based on the results from the above experiments, collision gas settings of 10 mL min^{-1} He and 6 mL min^{-1} D_2 were used for K isotope measurement. With these settings, the ArH^+ interference was kept below 0.2 mV, accounting for <0.03% of the $^{41}K^+$ signal. It is important to note that although the ArH^+ interference was also below 0.5 mV if 6 mL min^{-1} H_2 was used as a collision gas, K sensitivity was significantly lower in experiments using H_2 as a reaction gas (Fig. 2, plots A1 and B1), resulting in lower signal to noise ratios. The ArH^+ signal, when normalized to K sensitivity, was still higher than that in experiments using D_2 as the collision gas (Fig. 2, plot C1). Thus D_2 is slightly superior compared with H_2 for high precision K isotope analysis using collision cell MC-ICP-MS.

Based on measurement of an on-peak acid blank in all analytical sessions that used D_2 gas, ArH^+ interference typically varied by less than 7×10^{-5} volts over 12 hours. Between two analyses, ArH^+ interference variation was typically $<1.2 \times 10^{-5}$ volts, or 0.04‰ in $\delta^{41/39}K$; the maximum ArH^+ interference variation between two analyses was 3.4×10^{-5} volts, corresponding to 0.10‰ variation in $\delta^{41/39}K$. The analytical protocols developed in this study allow precise and accurate determination of $^{41}K/^{39}K$ ratios.

Isotope results and implications

Two sets of tests were performed to assess the accuracy of the analytical method. Test I used different amounts (20–150 μg) of a pure NIST SRM 3141a standard (for details, see Appendix†). Test II used synthetic samples, which were prepared by mixing pure 50 μg in-house K standard (UW-K) and K-free matrix elements to mimic real geological and biological samples (for details, see Appendix†). The K-free matrix elements were derived from the washes of samples that had been purified by an ion exchange column for K isotope analysis. These washes equate to approximately 3 mg of K-free rock powders, 20 mL of K-free river water, or 1 mg of K-free ashed biological samples. These two sets of test solutions were treated as unknowns, passed through ion exchange columns together with terrestrial samples and subsequently analyzed using the mass spectrometry procedures reported above. The measured $\delta^{41/39}K$ values for purified K from the Test I cluster were around 0‰ (−0.03 ± 0.13‰, 2SD, $n = 5$), whereas the measured $\delta^{41/39}K$ values for purified K from the Test II cluster were around −0.12‰ (−0.10 ± 0.08‰, 2SD, $n = 7$) (Fig. 3; Appendix†), consistent with the respective $\delta^{41/39}K$ values of NIST SRM 3141a (0‰) and UW-K (−0.12‰) within analytical uncertainty, confirming the accuracy of the whole procedure for samples with different matrices.

With the accuracy of the chemical and mass spectrometry procedures assured, we determined K isotope compositions for a variety of geological and biological samples (Fig. 3; Appendix†). The K isotope composition of seawater is nearly the same as that of NIST SRM 3141a; seawater $\delta^{41/39}K$ values vary between 0.02‰ and 0.12‰ for three replicate analyses of seawater. Four United States Geological Survey (USGS) igneous rock standards have very consistent $\delta^{41/39}K$ values that cluster around −0.5‰.

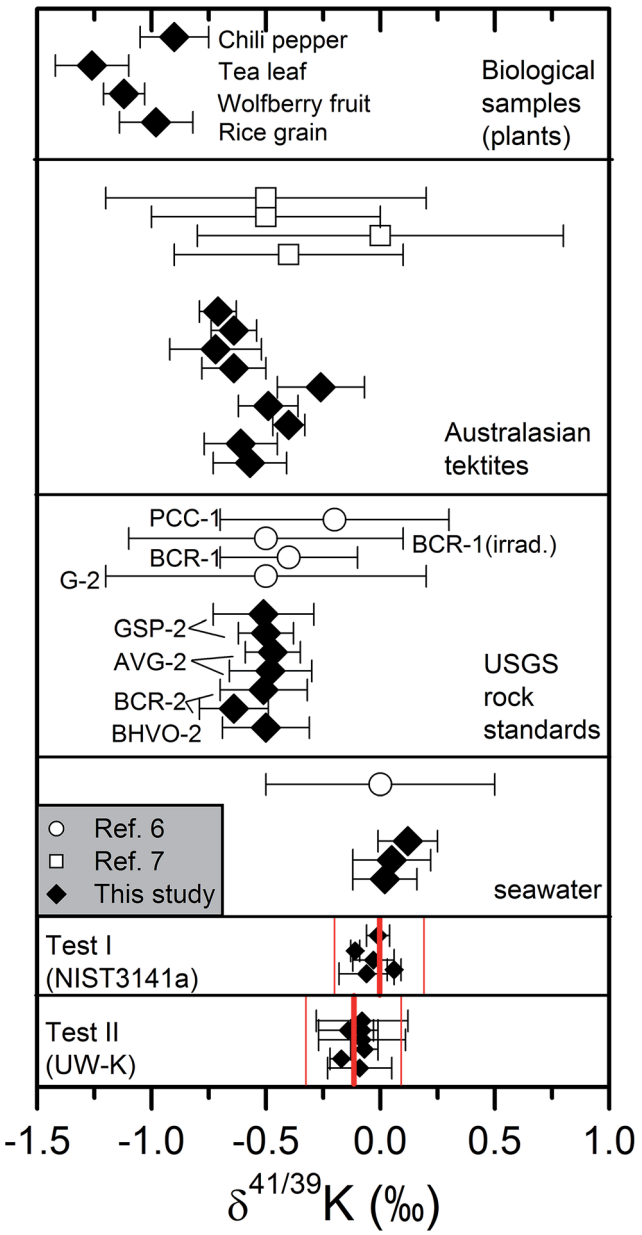

Fig. 3 Variations of $\delta^{41/39}K$ values in geological and biological samples. All data are reported against a NIST 3141a isotope standard. Black diamond (◆) denotes MC-ICP-MS data from this study, open circle (○) denotes SIMS data from ref. 6, and open square (□) denotes SIMS data from ref. 7. The error bar in this study represents 2 standard deviation of multiple analyses, and the error bar in SIMS analyses represents 2 standard error of multiple analyses.[6,7] The thick and thin red vertical lines denote the $\delta^{41/39}K$ values for the pure NIST SRM 3141a and UW-K solutions, and the external uncertainty of K isotope analysis.

The K isotope composition for seawater and selected USGS rock standards have been reported in a previous SIMS study,[6] but the data were reported against an in-house K solution from the University of Chicago. To allow comparison between the two studies, we arbitrarily set the University of Chicago in-house K solution to have a $\delta^{41/39}K$ value of −0.4‰ on the NIST 3141a scale, making seawater samples from the SIMS study and this study have comparable $\delta^{41/39}K$ values of ~0‰ (Fig. 3). Using this

scale, granite (G-2) and basalt (BCR-1) samples measured in the SIMS study have $\delta^{41/39}$K values of −0.4 to −0.5‰,[6,7] consistent with the $\delta^{41/39}$K values of granite (GSP-2), andesite (AVG-2), and basalt (BCR-2 and BHVO-2) measured in this study. However, it is important to note that the analytical error in previous SIMS studies[6,7] did not allow discrimination between K isotope compositions of rocks and seawater. This study, with significantly improved precision, shows that the isotopic difference between igneous rocks and seawater is resolvable.

Australasian tektites are a group of terrestrial debris ejected during a meteorite impact event about 0.786 million years ago;[23] a previous SIMS study suggested that Australasian tektites have K isotope compositions similar to terrestrial rocks[7] (Fig. 3). Analyses of Australasian tektites from southeast Asia and south China in this study (see sample description in the Appendix†) confirm the general consistency between Australasian tektites and USGS rock standards.

In addition, the K isotope compositions of leaves, seeds, and fruits of some plants have been determined. Plants have low $\delta^{41/39}$K values varying between −0.90‰ and −1.26‰ (Fig. 3). These low $\delta^{41/39}$K values stand in marked contrast compared to the source of the K that these plants would have used which would have ultimately been derived from igneous rocks. Similarly, significant isotopic fractionation of other metals such as Zn and Ni has been reported in plants.[24–26] The mechanisms for K isotope fractionation in plants remain to be explored.

The improved analytical precision provided by collision cell MC-ICP-MS enables confident discrimination of natural K isotope variation from terrestrial samples, which opens a new window for studying K-cycling. For example, weathering of silicate rocks is an important carbon sink that regulates atmospheric CO_2 levels and global changes; however, large uncertainties in the flux of CO_2 into continental sinks during silicate weathering stem from a lack of knowledge about the scale of neoformation of clay minerals in oceans and estuaries.[27] The higher $\delta^{41/39}$K value of seawater, as compared to crustal rocks, suggests significant K isotope fractionation during continental weathering and clay formation, making K isotopes a powerful tool for understanding K global cycling as well as CO_2 cycling. In addition, the remarkably low $\delta^{41/39}$K values found in higher plants implies that the biological uptake of K from the environment is accompanied by significant K isotope fractionation. Because K is a critical element for life that regulates many aspects of cell functionality, K isotopes may be used to probe K metabolism in different organisms and under different K uptake conditions (Fig. 3).

Conclusions

High precision measurement of ^{41}K/^{39}K ratios was achieved using a collision cell MC-ICP-MS, with collision gases of D_2 and He. Internal precision of <±0.07‰ (2SE) and external reproducibility of <±0.21‰ (2SD, or 95% confidence) in ^{41}K/^{39}K ratio measurement were achieved for purified geological and biological samples, which are improved values compared to the external precision of ±0.3‰ in collision cell MC-ICP-MS analyses using H_2 as the collision cell, and superior to the external precision of ±0.5‰ in SIMS and ±1‰ in TIMS analyses. With the improved precision, a ~1.3‰ variation in $\delta^{41/39}$K values among seawater, igneous rocks, and biological samples was identified, which implies that K isotope ratios may be used to study a variety of problems like continental weathering, global potassium cycling, and metabolism of potassium in organisms.

In addition to significantly improved precision, collision cell MC-ICP-MS requires much less sample for a K isotope measurement. Because there is no need to apply high mass resolution in collision cell MC-ICP-MS to avoid isobaric interferences, the instrument can run at full sensitivity, compared with reduced sensitivity in a conventional double focusing MC-ICP-MS without a collision cell.

We demonstrate that ArH^+ is generated in the plasma or in the interface region as well as in the collision cell but that the collision cell generated argon hydride can be suppressed from being formed by using D_2 as a reactive gas in the collision cell. The collision cell is a widely applied technique in quadruple ICP mass spectrometry; the isotopic labeling technique (*i.e.*, using D_2 as a reaction gas) proposed in this study provides new insights into molecule–ion interactions in a collision cell. Furthermore, although the MC-ICP-MS instrument (Micromass IsoProbe) used in this study is becoming obsolete, a new prototype of collision cell MC-ICP-MS is under development.[28] D_2 may be used as a collision gas in other future applications in which precision of isotopic ratios is strongly affected by hydride and hydroxide interference.

Acknowledgements

This study benefited from constructive comments from two anonymous reviewers. This study was supported by "1000-talent Program" of China to W. L. This study was also supported by the NASA Astrobiology Institute. This is publication No. 1 from Lunar and Planetary Science Institute, Nanjing University.

References

1 A. A. Verbeek and G. D. L. Schreiner, *Geochim. Cosmochim. Acta*, 1967, **31**, 2125.
2 G. D. L. Schreiner and A. A. Verbeek, *Proc. Roy. Soc. Lond. Math. Phys. Sci.*, 1965, **285**, 423.
3 E. L. Garner, L. A. Machalan and I. L. Barnes, *Proc. Lunar Planet. Sci. Conf.*, 1975, **6**, 1845–1855.
4 I. L. Barnes, E. L. Garner, J. W. Gramlich, L. A. Machlan, J. R. Moody, L. J. Moore, T. J. Murphy and W. R. Shields, *Proc. Lunar Planet. Sci. Conf.*, 1973, **2**, 1197–1207.
5 D. Wielandt and M. Bizzarro, *J. Anal. At. Spectrom.*, 2011, **26**, 366.
6 M. Humayun and R. N. Clayton, *Geochim. Cosmochim. Acta*, 1995, **59**, 2115.
7 M. Humayun and C. Koeberl, *Meteorit. Planet. Sci.*, 2004, **39**, 1509.
8 G. F. Herzog, C. M. O. D. Alexander, E. L. Berger, J. S. Delaney and B. P. Glass, *Meteorit. Planet. Sci.*, 2008, **43**, 1641.
9 K. E. Murphy, S. E. Long, M. S. Rearick and O. S. Ertas, *J. Anal. At. Spectrom.*, 2002, **17**, 469.

10 J. Sabine Becker and H.-j. Dietze, *J. Anal. At. Spectrom.*, 1998, **13**, 1057.
11 J. S. Becker, K. Fullner, U. D. Seeling, G. Fornalczyk and A. J. Kuhn, *Anal. Bioanal. Chem.*, 2008, **390**, 571–578.
12 S. J. Jiang, R. S. Houk and M. A. Stevens, *Anal. Chem.*, 1988, **60**, 1217.
13 C. M. Johnson, B. L. Beard and F. Albarède, *Geochemistry of Non-Traditional Stable Isotopes*, Mineralogical Society of America, St. Louis, Washington, DC, 2004.
14 J. G. Wiederhold, *Environ. Sci. Technol.*, 2015, **49**, 2606–2624.
15 L. E. Morgan, J. Higgins, B. Davidheiser-Kroll, N. S. Lloyd, J. Faithfull and R. M. Ellam, *Goldschmidt Conference Abstract*, 2014, p. 1731.
16 L. E. Morgan, N. S. Lloyd, R. M. Ellam and J. I. Simon, *AGU Fall Meeting Abstracts*, 2012, vol. 32, p. B2810.
17 D. Wollenweber, S. Strabburg and G. Wunsch, *Fresenius. J. Anal. Chem.*, 1999, **364**, 433–437.
18 F. M. Richter, R. A. Mendybaev, J. N. Christensen, D. Ebel and A. Gaffney, *Meteorit. Planet. Sci.*, 2011, **46**, 1152.
19 F. M. Richter, E. Bruce Watson, M. Chaussidon, R. Mendybaev, J. N. Christensen and L. Qiu, *Geochim. Cosmochim. Acta*, 2014, **138**, 136.
20 Z. Du and R. S. Houk, *J. Anal. At. Spectrom.*, 2000, **15**, 383.
21 M. Iglesias, N. Gilon, E. Poussel and J.-M. Mermet, *J. Anal. At. Spectrom.*, 2002, **17**, 1240.
22 S. D. Tanner, V. I. Baranov and D. R. Bandura, *Spectrochim. Acta, Part B*, 2002, **57**, 1361.
23 M. Trieloff, K. Bollinger, J. Kunz and E. K. Jessberger, *Meteorit. Planet. Sci.*, 2007, **42**, A150.
24 E. Smolders, L. Versieren, D. Shuofei, N. Mattielli, D. Weiss, I. Petrov and F. Degryse, *Plant Soil*, 2013, **370**, 605–613.
25 D. J. Weiss, T. F. D. Mason, F. J. Zhao, G. J. D. Kirk, B. J. Coles and M. S. A. Horstwood, *New Phytol.*, 2005, **165**, 703.
26 T.-H.-B. Deng, C. Cloquet, Y.-T. Tang, T. Sterckeman, G. Echevarria, N. Estrade, J.-L. Morel and R.-L. Qiu, *Environ. Sci. Technol.*, 2014, **48**, 11926.
27 P. Michalopoulos and R. C. Aller, *Science*, 1995, **270**, 614–617.
28 T. Elliott, H. Wehrs, C. Coath, J. Lewis and J. Schwieters, *Goldschmidt Conference Abstracts*, 2015, p. 824.